

가 , T1  
 T1  
 가  
 31 ( 21 , 10 , 8.7 )가  
 38 ( 18 , 16 , 4 )  
 T1 27 , 13  
 40 2 가  
 가 . 가 19 ( T1  
 14 , 5 ) ([SI<sub>lesion</sub> -  
 SI<sub>water</sub>]/[SI<sub>normal brain</sub> - SI<sub>water</sub>])  
 T1 10  
 ( 7 , 2 , 1 ) , 16 ,  
 ( 2 , 1 ) , 8 , 3  
 7 , 2 가  
 T1 (2.2±0.7,  
 2.2±0.6, p=0.914), (2.4±0.8, 4.5  
 ±1.5, p=0.018).

T1 , ,  
 가 , 가  
 가 .  
 (MRI) , .  
 (pulse sequence) , (con-  
 trast ratio) , T1  
 T1  
 (lesion conspicuity) 가  
 3 (0.3 mmol/kg b.w.) 가 (1, 2),  
 (magnetization transfer)  
 (3, 4).  
 T1 2000 3 2003 2 3  
 (5, 6).

2) 1, 3) , ,

가 31

38 가 21

가 10 , 1 18 ( 8.7

) . 38 18 , 16

4

1.5-T MR system (Magnetom Vision; Siemens Medical Systems, Iselin, NJ or Signa CV/i; GE Medical Systems, Milwaukee, Wis)

(Lesion Conspicuity)

T1

(acquisition time) (Table 1). 27 10

0.1 mmol/kg b.w. gadopentetate dimeglu- , 16

mine (Magnevist; Schering, Berlin, Germany) (Table 2).

4 T1 (Fig. 1) 7 , (Fig. 2) 2 ,

가 (Fig. 3) 1 ,

1

T1

(pair), 13 3

T1 27 , 8 , 2

13 40 (Table 3).

(lesion conspicuity) 2 (Fig. 4) 1 ,

(imaging artifact) 1 1

10 mm 가 (Imaging Artifact)

(contrast ratio) T1 14 , 3 , 5 , 7 (1

가 5

가 T1

가 2

가 (flow artifact)

(magnetization susceptibility artifact)

가 , 2

가 T1

가

Contrast ratio:  $[SI_{\text{lesion}} - SI_{\text{water}}] / [SI_{\text{normal brain}} - SI_{\text{water}}]$

가

**Table 2.** Qualitative Analysis for Lesion Conspicuity Between Post-contrast Fat-suppression Image and Postcontrast Conventional T1 Weighted Image

	Lesion Locations		
	Intra-axial	Extra-axial	Orbital
FS > Conventional	1*	7	2
FS = Conventional	11	4	1
FS < Conventional	1**	0	0

\*Fat-containing intra-axial tumor was easily characterized by post-contrast fat-suppression image.

\*\*Susceptibility artifact compromises the quality of fat-suppression image.

FS: Fat-suppression image

**Table 1.** Imaging Parameter and Acquisition Time of Variable Pulse Sequences

	Matrix	TR	TE	Flip angle	No. of slice	Thickness	Nex	Time (min)
Conv. T1	256 × 192	490 - 525	8 - 14	70 - 90 °	20	5	2	3.1
MT	256 × 192	525 - 602	8 - 14	70 - 90 °	20	5	2	5.3
FS	256 × 192	525 - 728	8 - 14	70 - 90 °	20	5	2	5.7

Conv. T1: Conventional T1 weighted imaging, MT: Magnetization Transfer, FS: Fat-suppression, TR: Repetition time, TE: Echo time, Time: Imaging acquisition time, Nex: Number of excitations

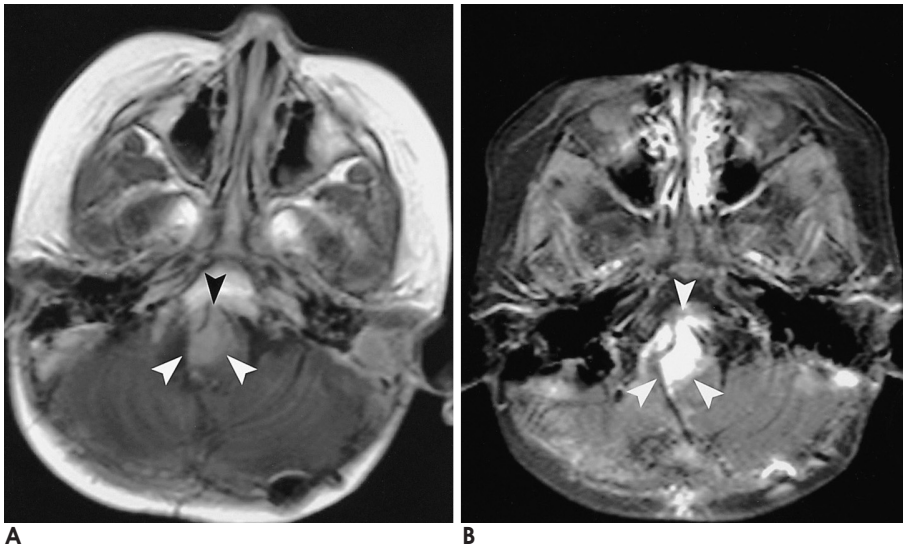


**Fig. 1.** A 2-year-old girl who underwent excision of infratentorial ependymoma. **A.** Postcontrast conventional T1-weighted image. A recurrent enhancing mass (arrowheads) located right lateral and anterior to the medulla is seen. The adjacent fatty marrow of skull base may decrease lesion conspicuity. **B.** Postcontrast fat-suppression image. Because high signal of fatty marrow was suppressed, the enhancing mass (arrowheads) is better delineated on postcontrast image than that of postcontrast conventional T1-weighted image. However, it shows more prominent signal loss due to magnetic susceptibility artifact around the mastoid bones than conventional T1-weighted image.

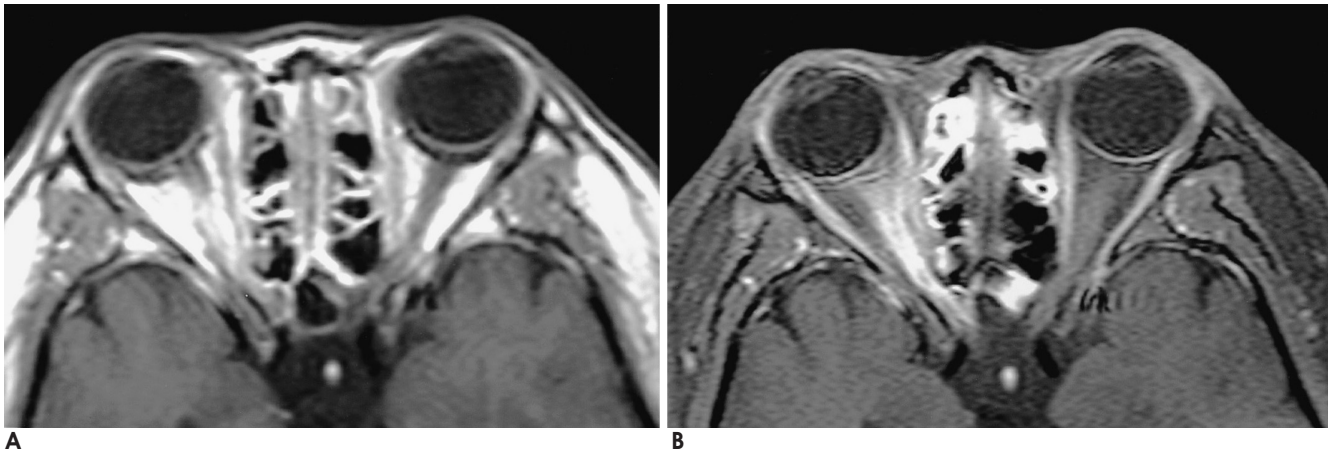


**Fig. 2.** A 16-year-old girl with optic neuritis. **A, B.** Enhancement of right optic nerve of postcontrast conventional T1-weighted image (**A**) is less conspicuous than that of postcontrast fat-suppression image (**B**) owing to suppressed signal of adjacent orbital fat.

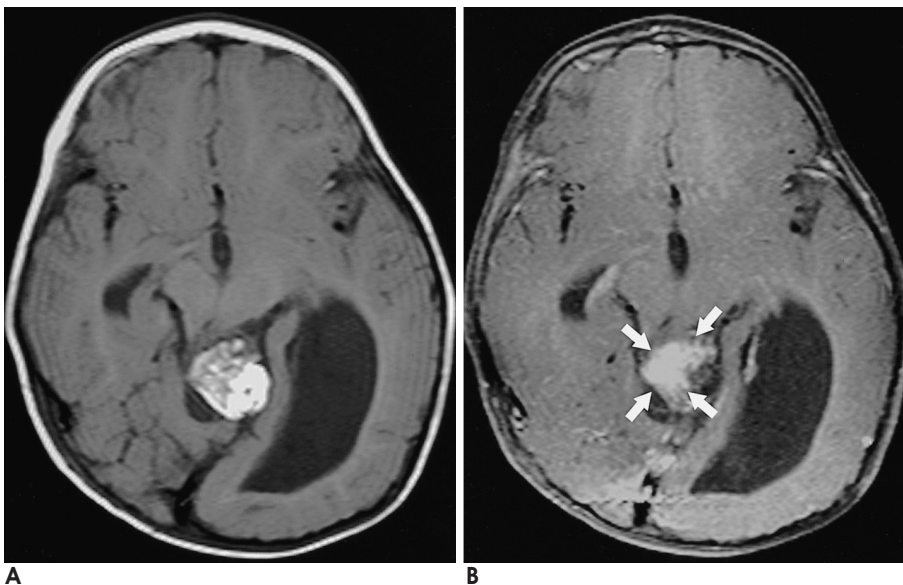


**Fig. 3.** An 1-year-old boy with lipoma in a pineal gland region. **A.** Precontrast conventional T1-weighted image cannot differentiate the high signal of tumor enhancing portion from that of the fat. **B.** Postcontrast fat suppression image specifically delineates the enhancing portion (arrows) of the tumor.

(Fig. 5).

(Contrast Ratio)

T1

**Table 3.** Qualitative Analysis for Lesion Conspicuity Between Postcontrast Fat-suppression Image and Postcontrast Magnetization Transfer Image

	Lesion Locations		
	Intra-axial	Extra-axial	Orbital
FS>MT	1	2	0
FS=MT	5	2	1
FS<MT	1	1	0

FS: Fat-suppression image, MT: Magnetization transfer image

가  
 (2.2±0.7, 2.2±0.6, p=0.914),  
 ±1.5, p=0.018) (Fig. 6).  
 (2.4±0.8, 4.5

가

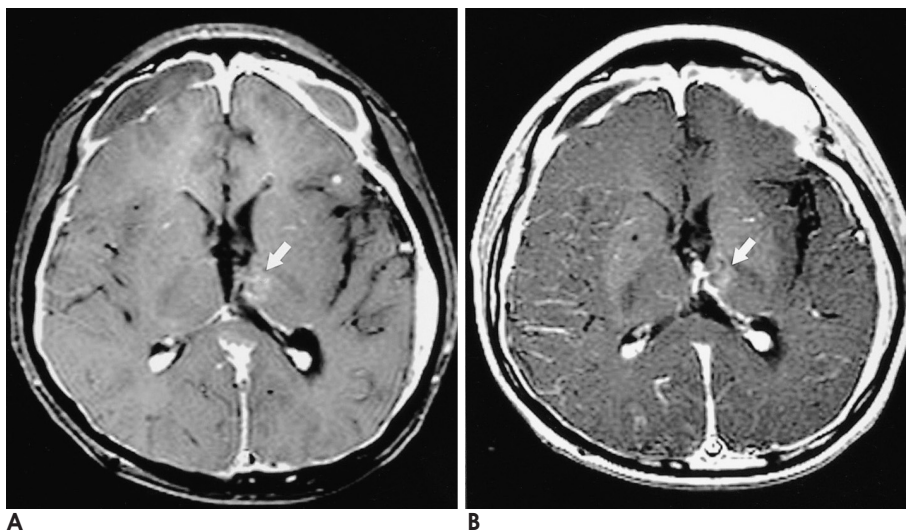


**Fig. 4.** A 13-year-boy who underwent excision of suprasellar mixed germ cell tumor.

**A.** Postcontrast fat-suppression image shows residual enhancing lesion (arrow) in the left thalamus.

**B.** Although postcontrast MT image also shows the enhancing (arrow) lesion in the left thalamus, the enhancing lesion is less conspicuous due to the adjacent bright basal ganglia and thalamus.

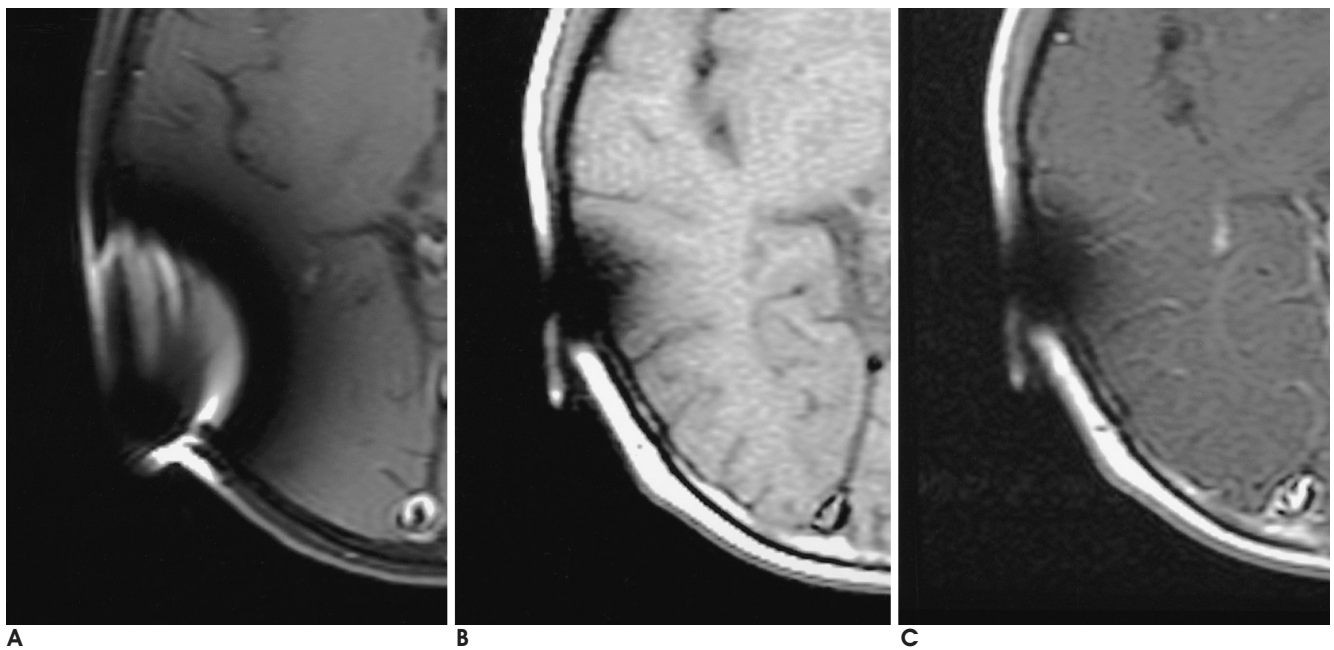


**Fig. 5.** A 10-year-old boy.

**A-C.** Magnetic susceptibility artifact is more exaggerated on fat-suppression image (A) than conventional T1-weighted (B) or MT (C) image.

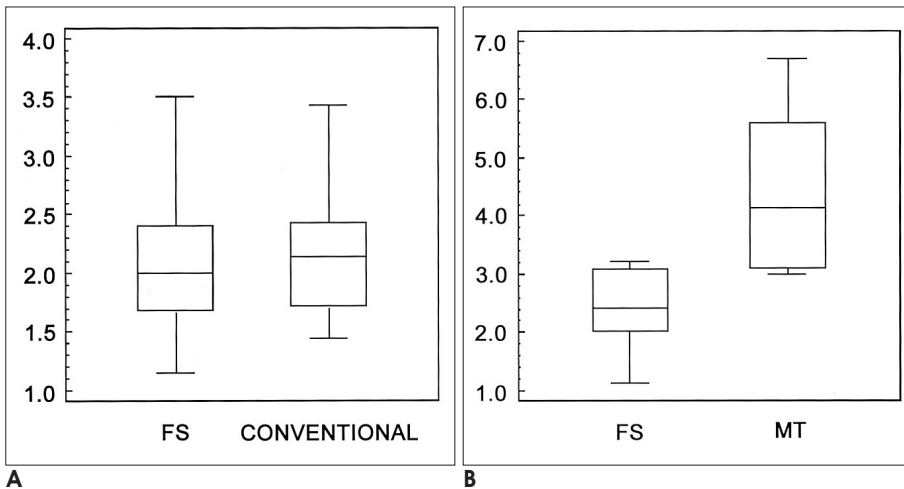


**Fig. 6.** Contrast ratios of paired post-contrast MR sequences.

**A.** The contrast ratio of postcontrast FS image and conventional T1-weighted image was comparable.

**B.** The contrast ratio of postcontrast MT image is higher than that of post-contrast FS image.

Note - FS: Fat-suppression, MT: Magnetization transfer.

가 가 가 (7).

31 5 (16.1%)

T1 (contrast - to - noise selection gradient (frequency - encoded view angle tilt - metal artifact reduction (10). (field inhomogeneities) magnetic field shimming, (11).

ratio)가 2 - 3 가 (3, 4). 가 2 (4.5 ± 1.5, 2.4 ± 0.8, p=0.018).

가 (central sulcus), (putamen), (substantia nigra), (caudate nucleus), (8).

T1 가 (orbit), (skull base), (neck), (spine), (5, 6). (intravestibular lipoma) (9).

T1 가 (Table 1), T1

T1

MR TR (repetition time)

가 ,  
 ,  
 T1  
 가 ,  
 가 , 1  
 ,  
 가  
 ,  
 ,  
 ,  
 ,  
 T1

1. Yuh WT, Fisher DJ, Engelken JD, Greene GM, Sato Y, Ryals TJ, et al. MR evaluation of CNS tumors: dose comparison study with gadopentetate dimeglumine and gadoteridol. *Radiology* 1991;180:485-491
2. Haustein J, Laniado M, Niendorf HP, Louton T, Beck W, Planitzer J, et al. Triple-dose versus standard-dose gadopentetate dimeglumine: a randomized study in 199 patients. *Radiology* 1993;186:855-

860

3. Finelli DA, Hurst GC, Gullapali RP, Bellon EM. Improved contrast of enhancing brain lesions on postgadolinium, T1-weighted spin-echo images with use of magnetization transfer. *Radiology* 1994;190:553-559
4. Mehta RC, Pike GB, Haros SP, Enzmann DR. Central nervous system tumor, infection, and infarction: detection with gadolinium-enhanced magnetization transfer MR imaging. *Radiology* 1995;195:41-46
5. Amano Y, Amano M, Kumazaki T. Normal contrast enhancement of extraocular muscles: fat-suppressed MR findings. *AJNR Am J Neuroradiol* 1997;18:161-164
6. Suenaga S, Abeyama K, Noikura T. Gadolinium-enhanced MR imaging of temporomandibular disorders: improved lesion detection of the posterior disk attachment on T1-weighted images obtained with fat suppression. *AJR Am J Roentgenol* 1998;171:511-517
7. Atlas SW. Rationale and clinical indications for contrast agents in MR imaging of the brain and spine. *J Comput Assist Tomogr* 1993;17:S1-S7
8. Elster AD, King JC, Mathews VP, Hamilton CA. Cranial tissues: appearance at gadolinium-enhanced and nonenhanced MR imaging with magnetization transfer contrast. *Radiology* 1994;190:541-546
9. Dahlen RT, Johnson CE, Harnsberger HR, Biediger CP, Syms CA, Fischbein NJ, et al. CT and MR imaging characteristics of intravestibular lipoma. *AJNR Am J Neuroradiol* 2002;23:1413-1417
10. Olsen RV, Munk PL, Lee MJ, Janzen DL, Mackay AL, Xiang QS, et al. Metal artifact reduction sequence: early clinical applications. *Radiographics* 2000;20:699-712
11. Tien RD, Hesselink JR, Chu PK, Szumowski J. Improved detection and delineation of head and neck lesions with fat suppression spin-echo MR imaging. *AJR Am J Neuroradiol* 1991;12:19-24

## Postcontrast T1-weighted Brain Magnetic Resonance Imaging in Pediatric Patients: Comparison Between Postcontrast Fat-suppression Imaging and Conventional T1-weighted or Magnetization Transfer Imaging<sup>1</sup>

Choong Wook Lee, M.D., Hyun Woo Goo, M.D.

<sup>1</sup>Department of Radiology, Asan Medical Center, University of Ulsan College of Medicine

**Purpose:** We wished to assess the merits and weaknesses of postcontrast fat-suppression (FS) brain MR imaging in children for the evaluation of various enhancing lesions as compared with postcontrast conventional T1-weighted or magnetization transfer (MT) imaging.

**Materials and Methods:** We reviewed the records of those patients with enhancing lesions on brain MR imaging who had undergone both FS imaging and one of the conventional T1-weighted or MT imaging as a post-contrast T1-weighted brain MR imaging. Thirty-one patients (21 male, 10 female; mean age, 8.7 years) with 38 enhancing lesions (18 intra-axial, 16 extra-axial and 4 orbital locations) were included in this study. There were 27 pairs of FS and conventional imagings, and 13 pairs of FS and MT imagings available for evaluation. Two radiologists visually assessed by consensus the lesions' conspicuity, and they also looked for the presence of flow or susceptibility artifacts in a total of 40 pairs of MR imagings. For 19 measurable lesions (14 pairs of FS and conventional T1-weighted imagings, 5 pairs of FS and MT imagings), the contrast ratios between the lesion and the normal brain ( $[SI_{lesion}-SI_{water}]/[SI_{normal\ brain}-SI_{water}]$ ) were calculated and compared.

**Results:** Compared with conventional imaging, the lesion conspicuity on FS imaging was better in 10 cases (7 extra-axial lesions, 2 orbital lesions and 1 fat-containing intra-axial lesion), equal in 16 cases, and worse in one case. Compared with MT imaging, the lesion conspicuity on FS imaging was better in 3 cases (2 extra-axial lesions and 1 intra-axial lesion), equal in 8 cases, and worse in 2 cases. Image quality of FS imaging was compromised by flow or susceptibility artifacts for 7 patients. The contrast ratios for FS imaging were not significantly different from those for conventional imaging ( $2.2 \pm 0.7$  vs.  $2.2 \pm 0.6$ , respectively,  $p=0.914$ ) and they were significantly lower than those for MT imaging ( $2.4 \pm 0.8$  vs.  $4.5 \pm 1.5$ , respectively,  $p=0.018$ ).

**Conclusion:** Postcontrast FS brain MR imaging appears to be better than the conventional T1-weighted imaging and comparable to MT imaging for the visual assessment of enhancing lesions. Especially, the FS imaging has the merit to delineate orbital and extra-axial enhancing lesions or fat-containing lesions, whereas it is disadvantageous when flow or susceptibility artifacts occur.

**Index words :** Children, central nervous system  
Brain, MR  
Magnetic resonance (MR), fat suppression  
Magnetic resonance (MR), pulse sequences  
Magnetic resonance (MR), technology

Address reprint requests to : Hyun Woo Goo, M.D., Department of Radiology, Asan Medical Center, University of Ulsan College of Medicine, 388-1 Poongnap2-dong, Songpa-gu, Seoul 138-736, Korea.  
Tel. 82-2-3010-4388 Fax. 82-2-476-4719 E-mail: hwgoo@amc.seoul.kr